

UCLA

UCLA Previously Published Works

Title

High-frequency oscillations in epileptic and non-epileptic Alzheimers disease patients and the differential effect of levetiracetam on the oscillations.

Permalink

<https://escholarship.org/uc/item/9jp031m2>

Journal

Brain Communications, 7(1)

Authors

Shandilya, M

Addo-Osafo, Kwaku

Ranasinghe, Kamalini

et al.

Publication Date

2025

DOI

10.1093/braincomms/fcaf041

Peer reviewed

BRAIN COMMUNICATIONS

High-frequency oscillations in epileptic and non-epileptic Alzheimer's disease patients and the differential effect of levetiracetam on the oscillations

 M. C. Vishnu Shandilya,¹  Kwaku Addo-Osafo,¹  Kamalini G. Ranasinghe,²
 Mohamad Shamas,¹  Richard Staba,¹  Srikantan S. Nagarajan² and Keith Vossel¹

Alzheimer's disease increases the risk of developing epilepsy together with cognitive decline. Early diagnosis or prediction of parameters associated with epileptic activity can greatly help in managing disease outcomes. Network hyperexcitability is a candidate of interest as a neurophysiological biomarker of Alzheimer's disease. High-frequency oscillations are increasingly recognized as potential biomarkers of hyperexcitability and epileptic activity. However, they have not yet been identified in Alzheimer's disease. In this study, we measured high-frequency oscillations via magnetoencephalography recordings in Alzheimer's disease patients with and without epileptic activity, as part of a Phase 2a randomized, double blind clinical trial of the efficacy of levetiracetam to improve cognitive functions in Alzheimer's disease. To measure the high-frequency oscillations, we used 10-min magnetoencephalography recordings (275-channel and sampling rate 1200–4000 Hz) during awake resting periods in participants with Alzheimer's disease and healthy controls. Recordings from 14 Alzheimer's disease participants, with six having non-epileptic Alzheimer's disease (median age: 60.8, 2 M/4 F), eight having sub-clinical epileptic activity (median age: 54.9, 5 M/3 F) and eight as control (median age: 71, 5 M/3 F), were analysed using two software scripts: Delphos and a custom-made script, for detecting high-frequency oscillations. Levetiracetam 125 mg twice-a-day or placebo was administered for 4 weeks in between two magnetoencephalography recordings, and 4 weeks of washout before switching levetiracetam/placebo phases for each participant. High-frequency oscillations were categorized into ripples (80 to 250 Hz) and fast ripples (250 to 500 Hz). At baseline, Alzheimer's disease participants, both epileptic and non-epileptic had higher rate of ripples and fast ripples than controls in several left/right hemispheric sensor regions ($P < 0.05$). Additionally, compared to epileptic, non-epileptic had higher rate of ripples in left-frontal, left-temporal and cerebral fissure regions and higher rate of fast ripples in left-frontal regions ($P < 0.05$). In epileptic type, levetiracetam decreased ripples in bilateral-frontal, bilateral-occipital regions and cerebral fissure, whereas in non-epileptic type, levetiracetam increased both ripples and fast ripples in right central and left parietal regions, and ripples in the right parietal region ($P < 0.05$). Additionally, we found hemisphere asymmetry in epileptic type, with right temporal/occipital having more high-frequency oscillations than their counterpart region. Overall, Alzheimer's disease had a high level of high-frequency oscillations, with higher numbers observed in non-epileptic type. Levetiracetam decreased high-frequency oscillations in epileptic but increased high-frequency oscillations in non-epileptic. Thus, high-frequency oscillations can function as a biomarker of hyperexcitability in Alzheimer's disease and may be more pathological when asymmetric and coinciding with presence of epileptic activity. Levetiracetam has the potential for treating hyperactivity in patients with epileptic Alzheimer's disease.

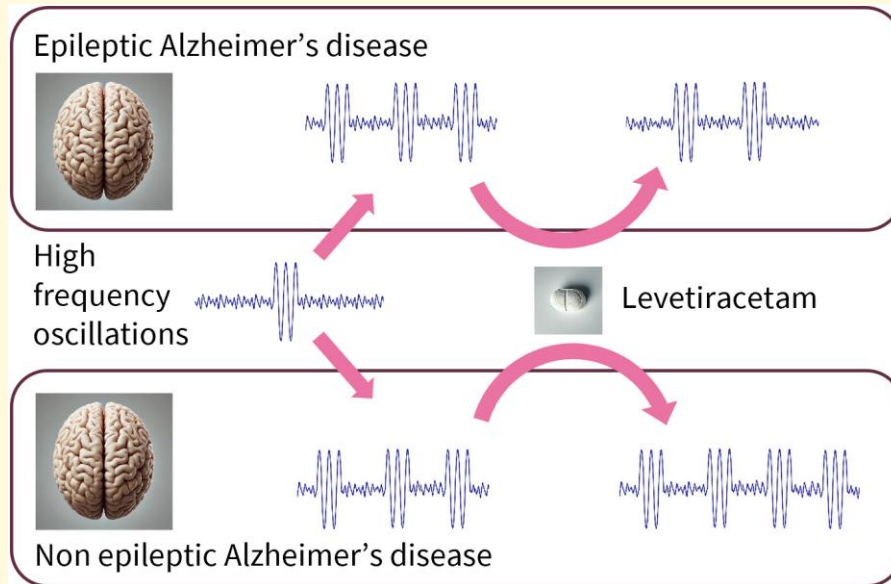
1 Department of Neurology, David Geffen School of Medicine, University of California, Los Angeles 90095, USA

2 Department of Radiology and Biomedical Imaging, University of California, San Francisco 94143, USA

Correspondence to: Keith Vossel, MD, MSc
 UCLA Department of Neurology, 710 Westwood Blvd
 Los Angeles, CA 90095, USA
 E-mail: kvossel@mednet.ucla.edu

Keywords: high-frequency oscillations; Alzheimer's disease; epilepsy; levetiracetam; hyperactivity

Graphical Abstract



Introduction

Having Alzheimer's disease increases the risk of developing epilepsy by around 3-fold,¹ with a significant proportion (23–62%) experiencing seizures in parallel with cognitive decline.^{2,3} Seizures also accelerate cognitive decline in Alzheimer's disease, and early diagnosis or prediction of parameters associated with epileptic activity can greatly help in managing disease outcomes.^{4,5} Anti-seizure medications can improve cognitive functions and may slow cognitive decline in patients with Alzheimer's disease and epileptic activity.^{4,6-8} Seizures and sub-clinical epileptic activity are a manifestation of neuronal network hyperexcitability,^{6,9} a state characterized by an imbalance between excitatory and inhibitory processes in the brain. Neuronal hyperexcitability can spread Alzheimer's disease pathology,¹⁰ and an early correction to reduce this activity correlates with reduced memory loss in mouse models of Alzheimer's disease.¹¹ Aberrant neuronal activity is also associated with early stages of Alzheimer's disease,¹² making it a candidate of interest as a neurophysiological biomarker.

There is a need for new biomarkers of hyperexcitability in Alzheimer's disease, as it is a treatable factor in cognitive decline associated with the disease. High-frequency oscillations

(HFOs) are increasingly recognized as potential biomarkers of hyperexcitability and epileptic activity.¹³⁻¹⁵ HFOs are observed both within and outside clinically defined seizure onset zones, with varying degrees of association to the epileptogenic zone (EZ),^{16,17} in both animal models and patients with refractory focal epilepsy^{18,19}; however, HFOs, particularly fast ripples (FR), in the EZ have more spectral power than those outside the zone,²⁰ and they are used to localize the EZ to improve surgical success in drug-resistant epilepsy patients.²¹ HFOs were originally discovered using microelectrode array recordings,²²⁻²⁵ and currently they are categorized by frequency into ripples (80–250 Hz) and FR (250–500 Hz).²⁶⁻²⁹ HFOs are spontaneous, rapid and transient brain waves, identifiable from the background signal, with clear patterns observed using intracranial recordings.^{15,16,30,31} Ripples (R) are associated with memory consolidation off-task,^{32,33} memory retrieval on-task,^{34,35} and represent inhibitory post-synaptic potentials.^{36,37} They can be both physiological and pathophysiological. When observed in intracranial EEG recordings, epileptic activity is more associated with R that occur on a flat background than those occurring on a non-flat background.³⁸ In contrast, FR are generally considered pathophysiological and associated with epileptic activity and atrophy,^{26,36,39-41} but their presence is observed in non-epileptic regions of

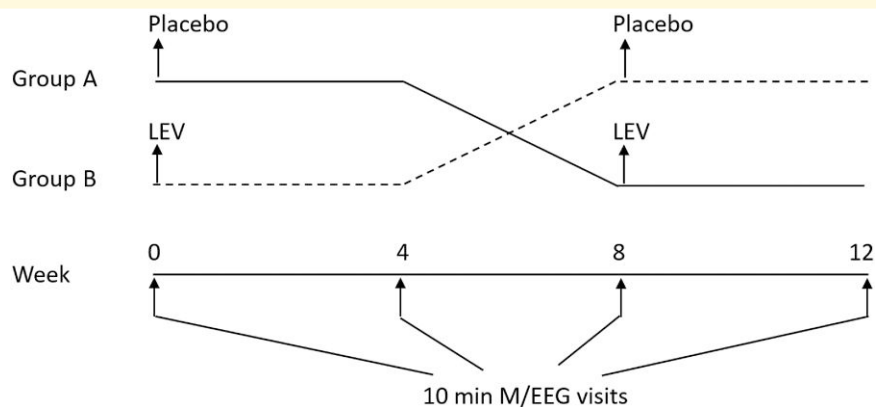


Figure 1 Switch-over treatment process. Alzheimer's disease participants had four 10-min MEG scans, with 4-week intervals between each scan. Controls had only one scan. Alzheimer's disease participants received either LEV 125 mg or placebo twice-a-day during the first 4 weeks and no treatment for the next 4 weeks. Then they received the opposite treatment (placebo or LEV) in the final 4 weeks.

epileptic patients.⁴² HFOs have been observed in both cortical and hippocampal regions, with potentially distinct functional roles. While hippocampal ripples are associated with memory consolidation, cortical ripples may be involved in local information processing and cross-regional communication.^{34,43} However, HFOs are yet to be identified in Alzheimer's disease. Scalp EEG and MEG recordings of HFOs have been reported in epilepsy including simultaneous recordings,⁴⁴ but have not been tested in Alzheimer's disease. If they are affected in Alzheimer's disease, they could become a potential neurophysiological biomarker of hyperexcitability in the disease. In this study, we examined HFOs using MEG in Alzheimer's disease patients with and without sub-clinical epileptic activity, which is a part of a Phase 2a randomized, double blind clinical trial of the efficacy of levetiracetam (LEV) to improve cognitive functions in Alzheimer's disease, in which HFOs were not examined. LEV was shown to improve the spatial memory and executive functions in patients with Alzheimer's disease and detectable epileptiform activity (EAD).⁴

Materials and methods

Study design and participants

The MEG recordings of Alzheimer's disease participants were derived from the previously published Vossel *et al.*⁴ study of LEV for Alzheimer's disease-associated network hyperexcitability. Briefly, it was a Phase 2a randomized double-blinded placebo-controlled crossover clinical trial conducted at the University of California, San Francisco (UCSF) and the University of Minnesota. It followed the Consolidated Standards of Reporting Trials (CONSORT) reporting guidelines for randomized clinical trials and was conducted in accordance with the Declaration of Helsinki.⁴⁵ Only data from UCSF were included for consistency in magnetoencephalography (MEG) recordings. Alzheimer's disease participants visited UCSF from October 16, 2014, to June 9, 2017. The

inclusion criteria include age less than 81; a diagnosis of probable Alzheimer's disease; a Mini-Mental State Examination (MMSE) score of 18 points or higher, and/or a Clinical Dementia Rating (CDR) score of <2 points. The exclusion criteria include participants receiving anti-seizure medications; significant systemic medical illness; and any condition, along with Alzheimer's disease, that could account for cognitive deficits. The MEG recordings of control participants were derived from the Vossel *et al.*⁴⁶ prospective observation clinical study. Controls were recruited between August 2008 and February 2015. The inclusion criteria include MMSE score of ≥ 28 ; a CDR-Sum of Boxes score of 0; no reports of cognitive deficits; and no atrophy less than that of age-appropriate level. Participants were grouped as Alzheimer's disease, Alzheimer's disease with EAD (spikes or sharp waves), Alzheimer's disease without epileptiform activity (NEAD), based on results from overnight EEG and 1-hour resting M/EEG exams or history of seizure (one Alzheimer's disease participant), and healthy controls. None of the controls had EAD on their overnight EEG or 1-hour resting M/EEG recordings. The data were analysed at the University of California, Los Angeles (UCLA) after August 2022.

M/EEG imaging

Participants underwent 10-min MEG recordings with simultaneous EEG (M/EEG, 275-channel) at high sampling rate (sampling rate 1200–4000 Hz) starting at 40 min into their 60-min resting-state, eyes-closed M/EEG exams. The recorded data are converted from CTF file system to EDF format (using *FieldTrip* MATLAB scripts) for visual inspection and for data processing in MATLAB. This generated 10 1-min EDF segments for MEG (275-channel) and EEG (21-channel) each, filed separately. Alzheimer's disease participants underwent four visits of M/EEG with 4 weeks of interval between each visit (Fig. 1). Controls visited only once.

Levetiracetam

Alzheimer's disease participants were randomly assigned to the switch-over treatment process (Fig. 1) where they initially received either LEV 125 mg twice-a-day or placebo for 4 weeks, followed by 4 weeks of washout (break period) and then received the opposite treatment for 4 weeks, or the reverse sequence. They had two M/EEG visits for each treatment stage, with 4-week intervals between them. Hence, total M/EEG visits are four. Controls were not administered LEV, and they only visited once for their M/EEG.

Data analysis

Among 17 Alzheimer's disease participants, we excluded their data from the analysis if they did not undergo all the four visits ($n=2$); their M/EEG sampling rate was <1000 Hz—which is required to detect HFOs ($n=2$); or if the recorded data was corrupted ($n=1$). Among 20 controls, 10 were randomly selected to match for sampling rate of M/EEG. Among these, we excluded the data from the analysis for those whose blood and cerebrospinal fluid sample was unavailable ($n=2$).

Initially, the EDF files were visually examined to check the presence of excessive noise, an abnormally high voltage that is present across multiple channels within a small period. As most of the files ($\sim 95\%$) do not have very high noise, no files were excluded at this stage. Then, the EDF files were processed by *Delphos detector* script,⁴⁷ which detects the HFOs by measuring the peaks in a signal and analyses them by the time width and frequency of the peaks above a threshold score that correspond to a normalized energy value. It begins by applying a Tukey window to reduce spectral leakage, and then calculates a time-frequency (TF) spectrogram. The algorithm removes outliers using interquartile range analysis and normalizes the data by fitting it to a normal distribution. It then employs image processing techniques to detect local maxima in the TF data by comparing each point in the TF data to its eight adjacent neighbours (i.e. time and frequency dimensions). Finally, it classifies these events as ripples or FR based on whether their local maxima fall within the pre-defined frequency bands for each type of oscillation (80–250 Hz for ripples, 250–500 Hz for FR). We set the threshold score to 20. Other standard settings used by the script are: minimum duration for HFO detection (1.4 times the expected oscillation period), maximum frequency spread for HFO (10 frequency divisions), frequency detail level in analysis (12 sub-divisions per doubling of frequency), TF resolution balance (set to 20, higher values favour frequency precision), analysed frequency range (3 octaves, covering 80–500 Hz) and threshold for identifying unusual signal patterns (0.005 for MEG data, where lower values are more selective). *Delphos* has high sensitivity and precision to detect HFOs even in low signal-to-noise ratio,⁴⁸ such as a MEG signal. The output gave a list of potential HFOs (candidates), which were then randomly verified visually. The output files that were

>400 kB (around 5% of total files), representing excessive noise, were excluded from further analysis (Supplementary Fig. S1). For the remaining files, we created an additional script in MATLAB to filter out noise by the following criteria: maximum five candidates across all channels within 400 ms, and the candidate with highest power among them was selected; the signal was high-pass filtered at 80 Hz and the standard deviation (SD) was calculated for signal's amplitude for each 400-ms time window. Most of the signals ($\sim 72\%$) were 1200 Hz; however, those that were higher were downsampled to 1200 Hz. The ratio of the candidate's maximum amplitude to the SD of its respective time window was calculated; candidates having ratios <3 were omitted as they had low amplitude of high-frequency component. HFO rates (averaged over 10-min recording) were analysed group-wise.

Sleep analysis

For determining awake or sleep from EEG, we filtered the signal using bandpass (1 to 40 Hz) filter and analysed the frequency of eye blinks as: awake if blinks were frequent, drowsy if blinks were occasional and their duration was >0.5 s, and stage-2 or stage-3 sleep if blinks were absent and the tracings had occasional, large amplitude, low frequency and synchronized waves.

Asymmetry index

We calculated Asymmetry index (AI) for EAD and NEAD to measure the degree of asymmetry of R and FR rates between hemispheres of brain. AI for was calculated using the formula: $AI = 200 * \frac{(\text{HFO rate left hemisphere} - \text{HFO rate right hemisphere})}{(\text{HFO rate left hemisphere} + \text{HFO rate right hemisphere})}$

We compared AI of EAD against NEAD to test the effect of epileptic factor and compared AI of both EAD and NEAD against zero for their respective group effect.

Statistical analysis

Fisher's test was used to analyse categorical variables. For MEG, the rate of R or FR, were grouped according to their respective lobar region. We calculated the average rate of R or FR of all participants within a cohort for each channel and compared regional channels between cohorts. For analysing absolute AI, we compared a group against a value of zero, using 2-tailed 1-sample Student's *t*-test. We checked normality of data using D'Agostino and Pearson test. For normally distributed data, for comparisons between two groups, we used 2-tailed unpaired Student's *t*-test (ST). For comparisons between three groups, we used ANOVA with Tukey's multiple comparisons test (AT). For data that was not normally distributed, we used Mann-Whitney test (MW) for two groups and Kruskal-Wallis test with Dunn's multiple comparisons test (KD) for three groups. We performed Spearman correlation analyses to assess the similarity across brain regions. For LEV analyzation, we

Table 1 Demographics of participants analysed

Characteristics	AD	EAD	NEAD	Control
<i>n</i>	14	8	6	8
Age, mean (SD), years	59.3 (6.3)	58.9 (7.0)	59.8 (5.8)	71.7 (4.7)
Male, No. (%)	7 (50)	5 (62.5)	2 (33.3)	5 (62.5)
Female, No. (%)	7 (50)	3 (37.5)	4 (66.7)	3 (37.5)
Education level, mean (SD), years	16.7 (3.4)	16.6 (4.1)	17.0 (2.7)	17.0 (1.1)
Handedness, right (%)	12 (85.7)	7 (87.5)	5 (83.3)	7 (87.5)
Race, white, No. (%)	14 (100)	8 (100)	6 (100)	8 (100)
Ethnicity, non-Hispanic, No. (%)	13 (92.8)	7 (87.5)	6 (100)	8 (100)
Acetylcholinesterase use (%)	14 (100)	8 (100)	6 (100)	0 (0)
Memantine use (%)	1 (7.1)	1 (12.5)	0 (0)	0 (0)
MMSE, mean (SD)	24.8 (3.2)	25.2 (2.0)	24.3 (4.6)	29.2 (0.8)
CDR, mean (SD)	0.64 (0.3)	0.62 (0.2)	0.66 (0.4)	0 (0)
CDR-SOB, mean (SD)	3.3 (1.4)	3.6 (0.7)	3.0 (1.9)	0 (0)
APOE ε4 carrier, <i>n</i> (%)	8 (57.1)	4 (50)	4 (66.6)	N/A

AD, Alzheimer's disease; EAD, epileptic AD; NEAD, non-epileptic AD; CDR, clinical dementia rating; SOB, sum of boxes.

compared drug versus placebo for each group. Analysis was performed using GraphPad Prism v10.2.

Results

Data demographics

The demographics of participants analysed are given in Table 1. There were 14 participants with Alzheimer's disease (eight EAD and six NEAD) and eight controls. In Alzheimer's disease, there were equal males (M) and females (F), with seven each. In controls, there were five M and three F. Sex was matched between Alzheimer's disease and controls ($P = 0.67$, Fisher's exact test). Sex was also matched between EAD, NEAD and controls ($P = 0.64$, Fisher's exact test). Controls (mean: 71.7 years) were 12.4 years older than Alzheimer's disease participants (mean: 59.3 years) ($P < 0.001$, unpaired t -test). Controls were 12.7 and 11.9 years older than EAD (mean: 58.9 years, $P = 0.001$) and NEAD (mean: 59.8 years, $P = 0.004$), respectively (ANOVA with Tukey's multiple comparisons test). Age was matched between EAD and NEAD ($P = 0.96$, ANOVA, Tukey's). Years of education were matched between Alzheimer's disease (mean: 16.79) and controls (mean: 17.0) ($P = 0.83$, unpaired t -test). Years of education were also matched between controls, EAD and NEAD (all $P > 0.96$, ANOVA, Tukey's). Self-identified race and ethnicity of all the participants was white and non-Hispanic/Latinx, respectively. There was no significant difference between sampling rates of MEG recordings between Alzheimer's disease and control ($P = 0.12$) and between EAD and NEAD ($P = 0.17$, unpaired t -tests). There were no significant differences between control versus Alzheimer's disease and EAD versus NEAD for handedness ($P > 0.99$) or memantine use ($P > 0.99$) (Fisher's exact test). All Alzheimer's disease participants used acetylcholinesterase inhibitors. EAD (mean: 25.25, $P = 0.022$) and NEAD (mean: 24.33, $P = 0.009$) had lower MMSE scores than controls (mean: 29.25), but no difference between them ($P = 0.81$, ANOVA, Tukey's). No differences were found between EAD and NEAD for CDR ($P = 0.81$) or CDR-Sum of Boxes ($P = 0.38$) (unpaired t -tests).

Eight (57.1%) Alzheimer's disease patients were APOE ε4 carriers, with no significance difference between EAD and NEAD groups ($P = 0.62$, Fisher's exact test).

MEG signal characteristics

M/EEG signal had high power at multiples of 60 Hz, indicating the presence of strong electrical noise interference from the power lines or other electronic devices operating at the same frequency. Moreover, while the detected HFO events could be differentiated from the background noise, their prominence was not exceptional, indicating low signal-to-noise ratio. *Delphos detector* identified several oscillations as HFOs. We additionally filtered out the oscillations that had their peak values < 3 SD relative to the signal (Supplementary Fig. S2 shows filtered out samples). Figures 2 and 3 illustrates ripples and FR, respectively, from the right temporal region of an EAD participant. Additional example HFOs (R and FR) are shown in Supplementary Fig. S3. Supplementary Fig. S4 shows spatial specificity of a typical HFO. Simultaneous EEG data had low signal-to-noise and was thus excluded from HFO analysis. In our study, four participants were awake, 14 were drowsy (Stage 1 sleep) and 4 were in Stage 2 sleep during the 10-min recordings, with no significant difference between controls, EAD and NEAD ($P > 0.99$, Fisher's exact test). Spearman correlation analysis revealed a range of correlations for rate of ripples from -0.30 to 0.47 across the 11 brain regions, with a median of 0.01 and interquartile range from -0.11 to 0.10 . For FR, the range was from -0.48 to 0.39 , median of 0.00 and interquartile range from -0.11 to 0.15 . This indicated that most correlations were weak, suggesting relative independence among most brain regions.

Alzheimer's disease participants have more ripples and fast ripples than controls

MEG detected higher average ripple rate (RR) in Alzheimer's disease compared to controls (CN) in the left central

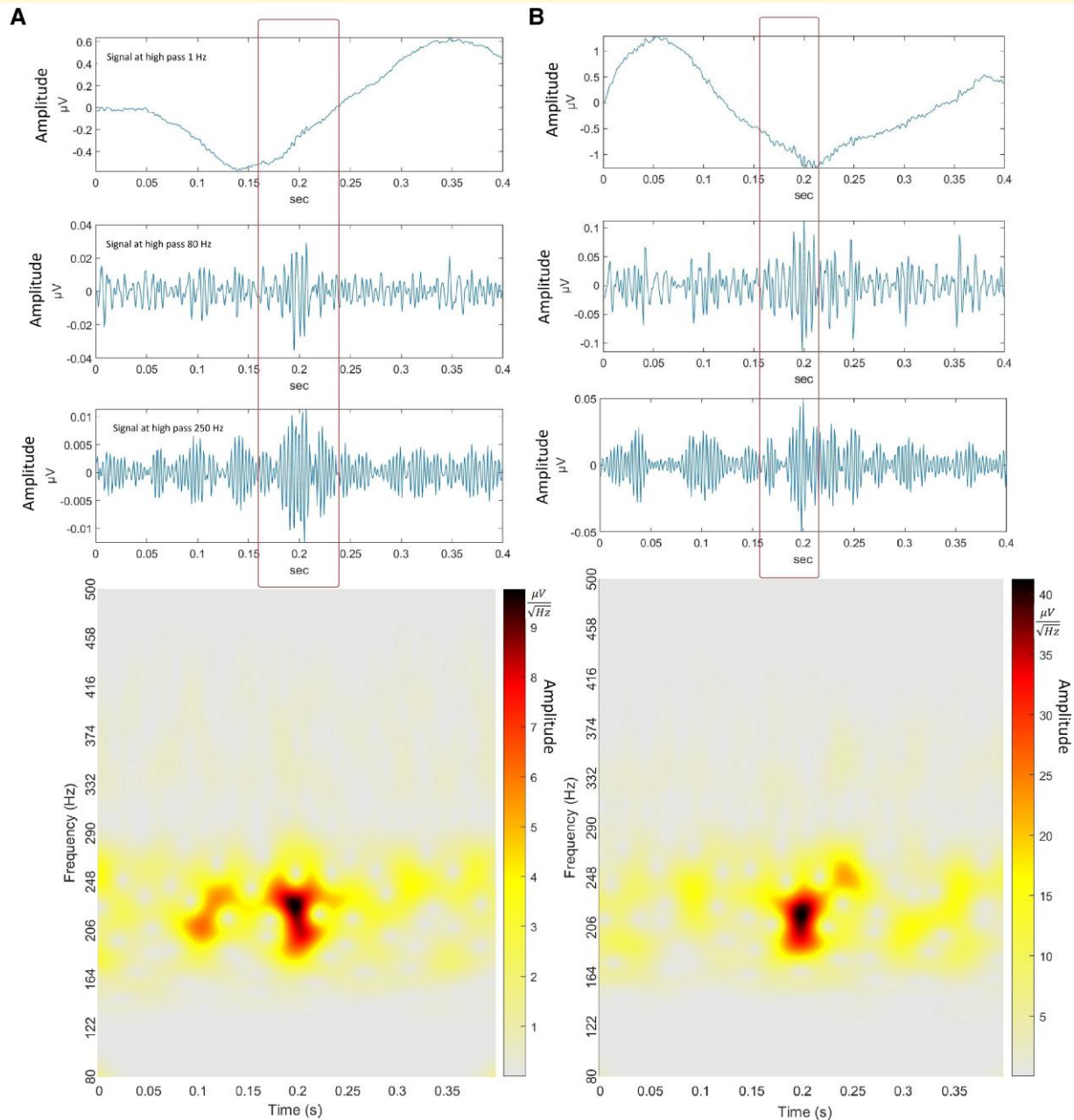


Figure 2 Typical MEG ripples detected by Delphos detector software. (A) Ripple 200 Hz at right temporal-44 channel and **(B)** ripple 212 Hz at left temporal-51. Top to bottom for each HFO: Signals with high-pass filter at 1, 80 and 250 Hz, and spectrogram of the above signal segment.

(Alzheimer's disease = 7.49, CN = 4.28, $P < 0.0001$, MW), left parietal (Alzheimer's disease = 8.99, CN = 4.33, $P < 0.0001$, ST), left temporal (Alzheimer's disease = 14.78, CN = 8.60, $P = 0.0001$, ST), right occipital (Alzheimer's disease = 12.67, CN = 6.63, $P < 0.0001$, ST), right parietal (Alzheimer's disease = 12.87, CN = 6.61, $P < 0.0001$, ST), right temporal (Alzheimer's disease = 21.95, CN = 13.01, $P < 0.0001$, ST) and cerebral fissure (Alzheimer's disease = 13.30, CN = 8.25, $P = 0.04$, ST) regions (Fig. 4A). Alzheimer's disease participants had higher average FR rate (FRR) than controls in the left central (Alzheimer's disease = 1.79, CN = 0.84,

$P < 0.0001$, ST), left frontal (Alzheimer's disease = 2.15, CN = 1.35, $P = 0.04$, MW), left parietal (Alzheimer's disease = 1.81, CN = 0.92, $P = 0.0059$, MW), left temporal (Alzheimer's disease = 2.96, CN = 1.84, $P = 0.0015$, MW), right central (Alzheimer's disease = 1.80, CN = 1.16, $P = 0.036$, ST), right frontal (Alzheimer's disease = 2.49, CN = 1.59, $P = 0.0021$, MW), right occipital (Alzheimer's disease = 3.20, CN = 1.14, $P < 0.0001$, ST), right parietal (Alzheimer's disease = 2.36, CN = 1.47, $P = 0.01$, ST), right temporal (Alzheimer's disease = 3.97, CN = 1.74, $P < 0.0001$, MW) and cerebral fissure (Alzheimer's disease =

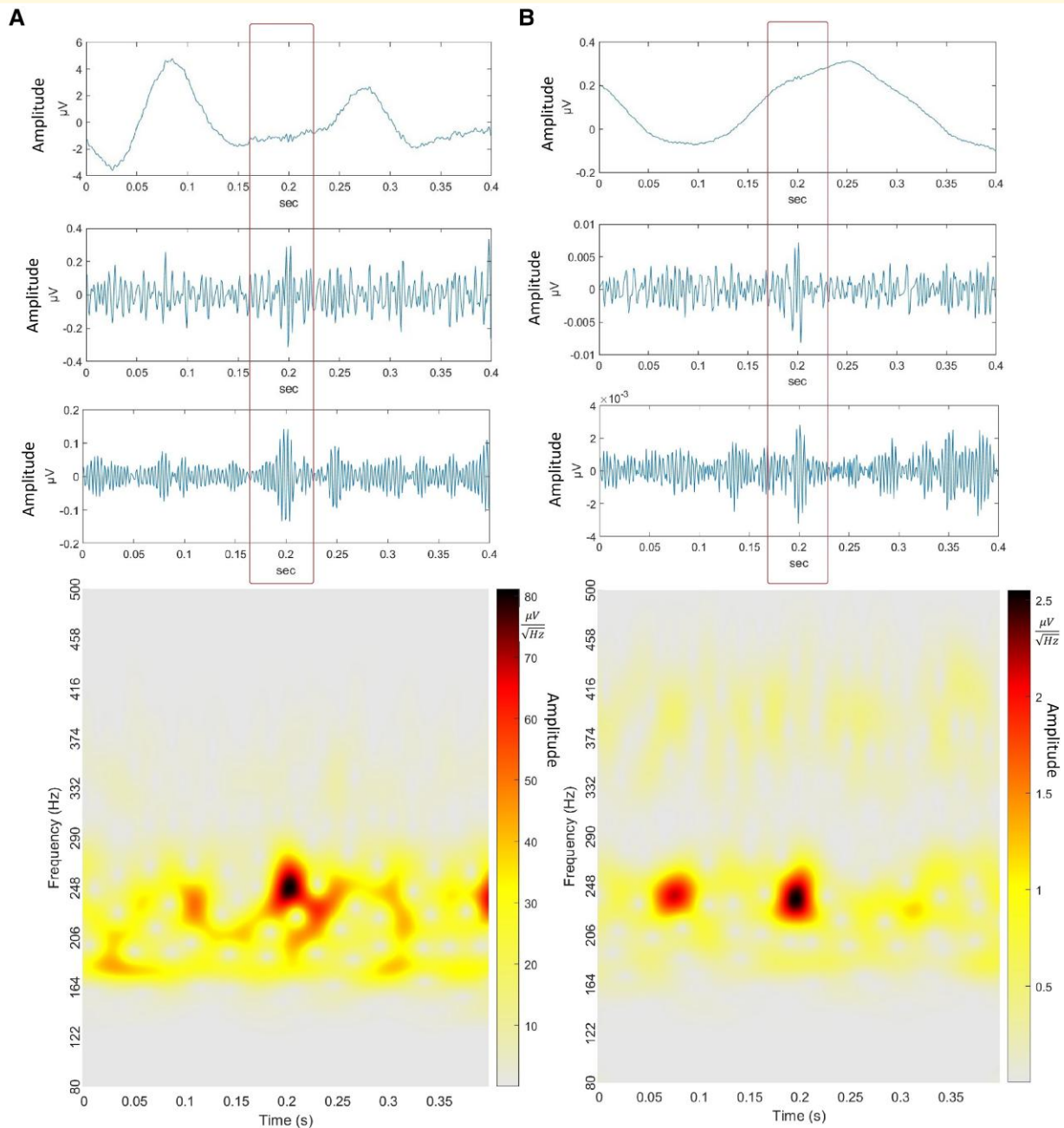


Figure 3 Typical MEG FR detected by Delphos detector software. (A) FR 267 Hz at right frontal-13. **(B)** FR 252 Hz at left temporal-31. Top to bottom for each HFO: Signals with high-pass filter at 1, 80 and 250 Hz, and spectrogram of the above signal segment.

2.25, $CN = 0.89$, $P = 0.003$, ST) regions (Fig. 4B). FR occurred in more lobes than R. Both R and FR were most frequent in right temporal and right occipital regions.

Both EAD and NEAD participants have higher rates of ripples and fast ripples than controls

MEG detected higher RR in EAD than controls in the left central (EAD = 7.07, $CN = 4.28$, $P = 0.015$, KD), left

parietal (EAD = 7.81, $CN = 4.33$, $P = 0.016$, KD), right occipital (EAD = 12.49, $CN = 6.63$, $P = 0.0003$, AT), right parietal (EAD = 12.19, $CN = 6.61$, $P = 0.0018$, KD) and right temporal (EAD = 21.27, $CN = 13.01$, $P = 0.0001$, AT) regions (Fig. 5A). NEAD had higher RR than controls in the left central ($CN = 4.28$, NEAD = 8.04, $P = 0.008$, KD), left frontal ($CN = 8.38$, NEAD = 14.38, $P = 0.005$, KD), left parietal ($CN = 4.33$, NEAD = 10.54, $P < 0.0001$, KD), left temporal ($CN = 8.59$, NEAD = 19.00, $P < 0.0001$, AT), right occipital ($CN = 6.63$, NEAD = 12.89, $P < 0.0001$, AT), right parietal ($CN = 6.61$, NEAD = 13.77, $P < 0.0001$, KD)

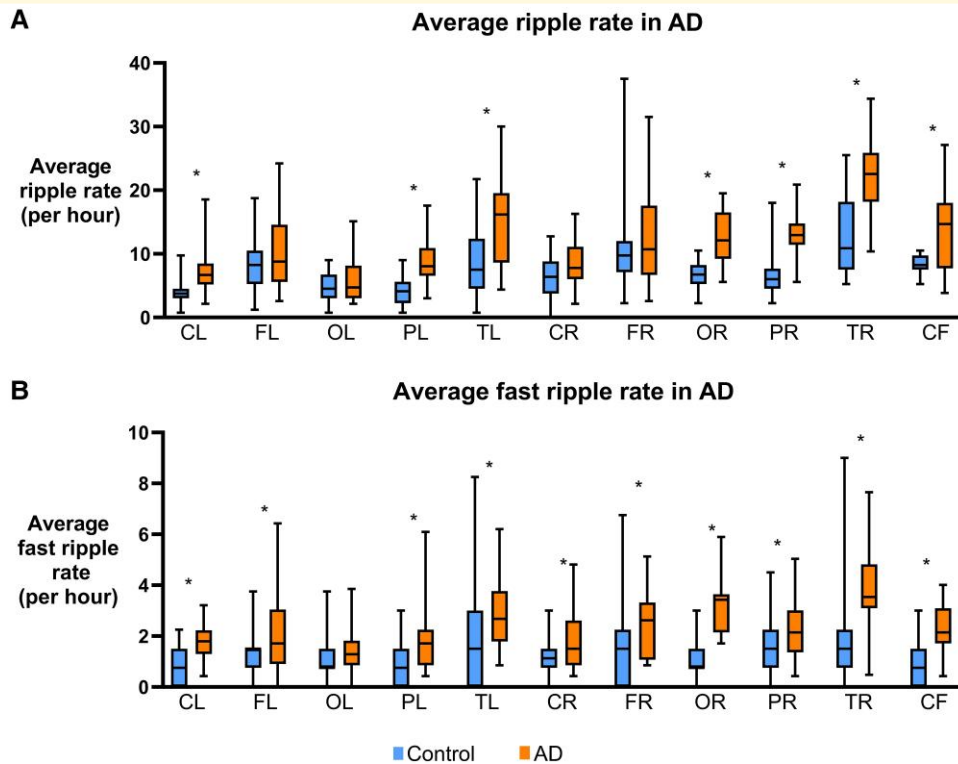


Figure 4 HFOs in Alzheimer's disease. (A) Average RRs per region detected in MEG for Alzheimer's disease are shown in box plot. Alzheimer's disease had higher RR than controls in central, parietal and temporal regions, and cerebral fissure. (B) Average FRR per region detected in MEG for Alzheimer's disease are shown in box plot. Alzheimer's disease had higher FRR than controls in all regions except left occipital. $P < 0.05$, Student's *t*-test or Mann-Whitney test. The average RR or FRR of all participants within a cohort is calculated for each channel, and each regional group of channels is compared between cohorts. Number of channels (**N**) for each region are as follows: CL, central left ($n = 24$); FL, frontal left ($n = 31$); OL, occipital left ($n = 19$); PL, parietal left ($n = 22$); TL, temporal left ($n = 33$); CR, central right ($n = 24$); FR, frontal right ($n = 33$); OR, occipital right ($n = 19$); PR, parietal right ($n = 22$); TR, temporal right ($n = 34$); CF, cerebral fissure ($n = 11$).

and right temporal (CN = 13.01, NEAD = 22.85, $P < 0.0001$, AT) regions. Surprisingly, NEAD had higher RR than EAD in the left frontal (EAD = 7.57, NEAD = 14.38, $P = 0.0001$, KD), left temporal (EAD = 11.61, NEAD = 19.00, $P < 0.0001$, AT) and cerebral fissure (EAD = 9.56, NEAD = 18.27, $P = 0.037$, KD) regions.

EAD had higher FRR than controls in the left central (EAD = 1.82, CN = 0.84, $P = 0.0035$, AT), right occipital (EAD = 3.11, CN = 1.14, $P = 0.0005$, AT) and right temporal (EAD = 3.58, CN = 4.47, $P = 0.0002$, KD) regions (Fig. 5B). NEAD had higher FRR than controls in the left central (CN = 0.84, NEAD = 1.75, $P = 0.007$, AT), left frontal (CN = 1.35, NEAD = 2.87, $P = 0.003$, KD), left parietal (CN = 0.92, NEAD = 2.31, $P = 0.013$, KD), left temporal (CN = 1.84, NEAD = 3.39, $P = 0.001$, KD), right frontal (CN = 1.59, NEAD = 2.78, $P = 0.0017$, KD), right occipital (CN = 1.14, NEAD = 3.31, $P < 0.0001$, AT), right parietal (CN = 1.46, NEAD = 2.63, $P = 0.022$, AT), right temporal (CN = 1.74, NEAD = 4.47, $P < 0.0001$, KD) and cerebral fissure (CN = 0.88, NEAD = 2.72, $P = 0.015$) regions. NEAD had higher FRR than EAD in the left-frontal (EAD = 1.64, NEAD = 2.87, $P = 0.025$) region.

LEV decreased ripples in EAD, but increased ripples and fast ripples in NEAD

In Alzheimer's disease, LEV decreased R in the left frontal ($P < 0.0001$) and right occipital ($P = 0.017$) regions and increased R in the left parietal ($P < 0.0001$), right parietal ($P = 0.0003$) and right central ($P = 0.0007$) regions (Fig. 6A). In EAD, LEV decreased R in the left frontal ($P < 0.0001$, ST), right frontal ($P = 0.013$, ST), left occipital ($P = 0.036$, ST), right occipital ($P = 0.002$, MW) and cerebral fissure ($P = 0.009$, ST) regions (Fig. 6B). However, in NEAD, LEV increased R in the left parietal ($P < 0.0001$, ST), right parietal ($P = 0.0002$, MW) and right central ($P < 0.0001$, ST) regions (Fig. 6C).

In Alzheimer's disease, LEV decreased FR in right temporal region ($P = 0.03$, ST) but increased them in cerebral fissure ($P = 0.02$, MW) (Fig. 7A). For FR, in EAD, LEV did not show any effect (Fig. 7B). In NEAD, LEV increased FR in the left parietal ($P = 0.006$) and right central ($P = 0.035$) regions (ST) (Fig. 7C); both regions showed increase in R too.

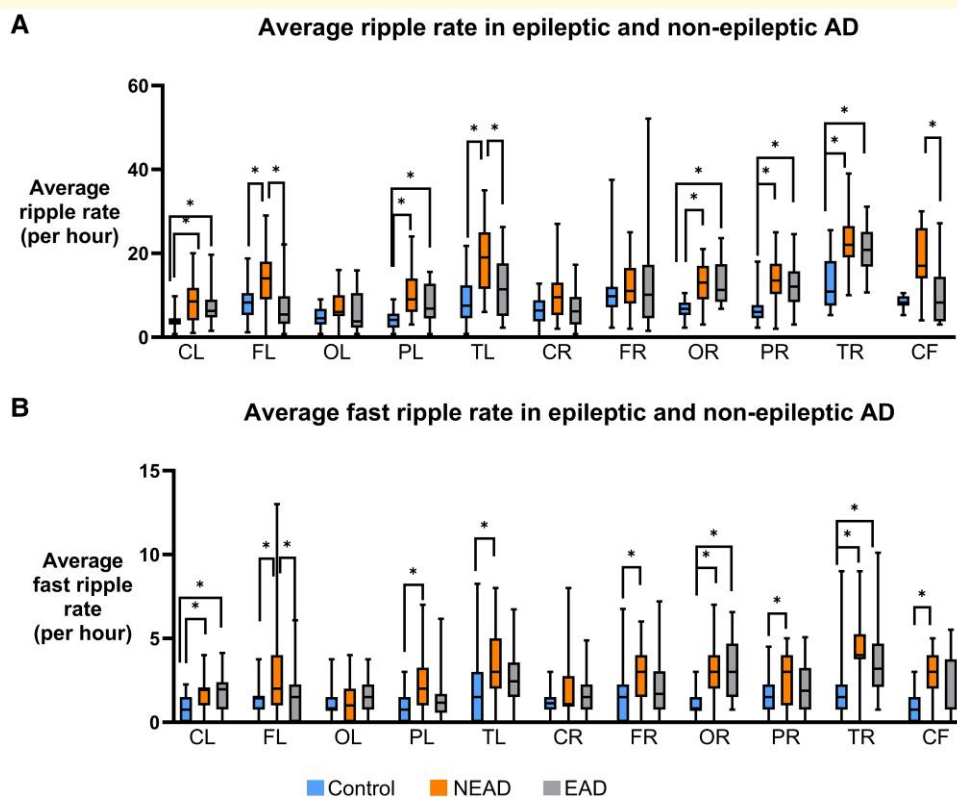


Figure 5 HFOs in epileptic and non-epileptic Alzheimer's disease. (A) Average RRs per region detected in MEG for EAD and NEAD are shown in box plot. EAD had higher RR than controls in left central, left parietal, right occipital, right parietal and right temporal regions. NEAD had higher RR than controls in all regions except left occipital and right frontal. NEAD had higher RR than EAD in left frontal, left temporal and cerebral fissure. (B) Average FRR per region detected in MEG for EAD and NEAD are shown in box plot. EAD had higher FRR than controls in left central, right occipital and right temporal regions. NEAD had higher FRR than controls in all regions except left occipital and right central. NEAD had higher FRR than EAD in left-frontal region. $P < 0.05$, one-way ANOVA/Tukey or Kruskal–Wallis test with Dunn's multiple comparisons test. The average RR or FRR of all participants within a cohort is calculated for each channel, and each regional group of channels is compared between cohorts. Number of channels (**N**) for each region are as follows: CL, central left ($n = 24$); FL, frontal left ($n = 31$); OL, occipital left ($n = 19$); PL, parietal left ($n = 22$); TL, temporal left ($n = 33$); CR, central right ($n = 24$); FR, frontal right ($n = 33$); OR, occipital right ($n = 19$); PR, parietal right ($n = 22$); TR, temporal right ($n = 34$); CF, cerebral fissure ($n = 11$).

Asymmetry index of HFOs

EEG showed epileptic activity in the bilateral frontal region ($n = 1$) and predominantly left temporal region ($n = 5$) for EAD participants, where MEG showed bilateral temporal ($n = 1$) and left temporal ($n = 1$) epileptic activity. A patient in the EAD group had a recent history of seizures but no epileptic activity during M/EEG recording. We compared AI of EAD against the AI of NEAD. There was no significant difference between AIs of EAD and NEAD for both R (P value for regions is 0.79 for central, 0.50 for frontal, 0.81 for occipital, 0.61 for parietal, 0.07 for temporal and 0.30 for whole hemisphere) and FR (P value for regions is 0.92 for central, 0.63 for frontal, 0.55 for occipital, 0.27 for parietal, 0.67 for temporal and 0.66 for whole hemisphere; ST). We also compared AI of EAD and NEAD against zero for assessing absolute asymmetry. We found higher R in the right hemisphere for EAD in the temporal region ($P = 0.005$; 1-sample t -test). There was no asymmetry for R in NEAD. We found higher FR in the right hemisphere for EAD in

the occipital region ($P = 0.015$; 1-sample t -test). There was no asymmetry for FR in NEAD (Fig. 8).

Discussion

HFOs have so far not been observed in MEG recordings that are not associated with epilepsy until now. In this study, we showed that Alzheimer's disease exhibits more R and FR in several brain regions. This finding is in line with the current view that neuronal hyperactivity is associated with Alzheimer's disease.³ We also noted that FR occur in more lobes than R in Alzheimer's disease, which is in line with the view that FR are more often pathological and expected to be more pronounced in disease conditions.²⁹ Several regions showed more HFOs in Alzheimer's disease; however, not all lobes were affected to the same degree. The right temporal and right occipital regions showed greater difference than controls in both R and FR. This could be due to the pathological process, including tauopathy, affecting the

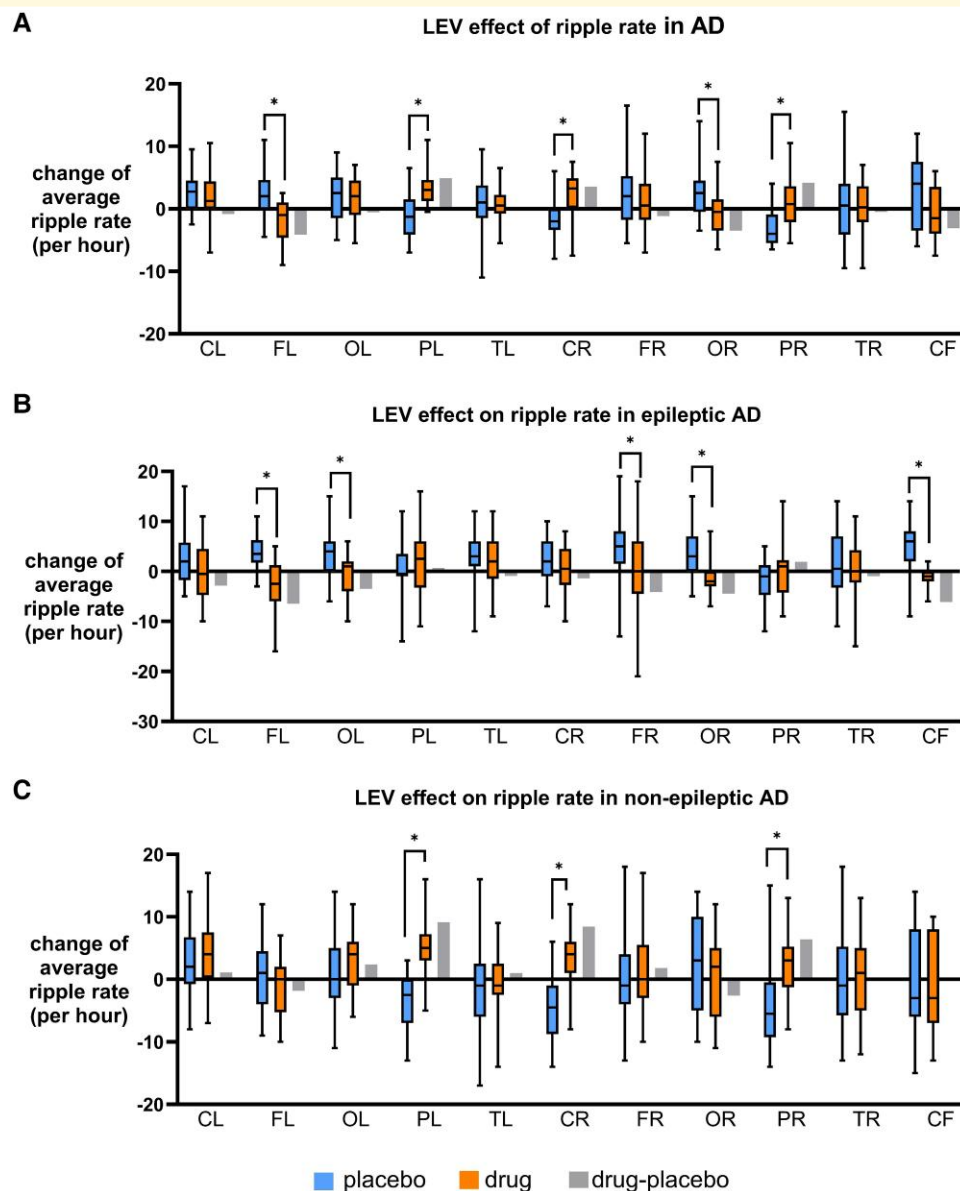


Figure 6 Effect of LEV on ripples. (A) Average RRs per region detected in MEG for Alzheimer's disease before and after LEV treatment are shown in box plot. LEV increased RR in Alzheimer's disease in bilateral parietal and right central but decreased RR in left-frontal and right-occipital regions. (B) Average RRs per region detected in MEG for EAD before and after LEV treatment are shown in box plot. In EAD, LEV decreased RR in bilateral-frontal and occipital regions and cerebral fissure. (C) Average RRs per region detected in MEG for NEAD before and after LEV treatment are shown in box plot. In NEAD, LEV increased RR in bilateral parietal and right central regions. $P < 0.05$, unpaired t -test or Mann-Whitney test. The average RR or FRR of all participants within a cohort is calculated for each channel, and each regional group of channels is compared between cohorts. Number of channels (**N**) for each region are as follows: CL, central left ($n = 24$); FL, frontal left ($n = 31$); OL, occipital left ($n = 19$); PL, parietal left ($n = 22$); TL, temporal left ($n = 33$); CR, central right ($n = 24$); FR, frontal right ($n = 33$); OR, occipital right ($n = 19$); PR, parietal right ($n = 22$); TR, temporal right ($n = 34$); CF, cerebral fissure ($n = 11$).

region in the early stages and spreading to rest of the brain,⁴⁹ implying that tauopathy could influence the prevalence or intensity of HFOs in affected brain regions. Our results also confirm the findings in mouse models that showed Alzheimer's disease and epilepsy models had higher HFOs than controls.⁵⁰ Additionally, the dentate gyrus showed robust HFO activity in mouse models, which is similar to the temporal lobe having higher HFOs in our study. NEAD

had higher HFO rates than EAD in a few regions. We hypothesize that compensatory alterations in metabolic activity and molecular expressions, for example, relatively higher levels of neuropeptide Y,^{51,52} can reduce wider network hypersynchrony in these cases. We found significant asymmetry of HFOs in EAD, but not in NEAD. EAD had higher HFO rates, for both R (in occipital and temporal regions) and FR (in occipital region), in the right hemisphere. This is in

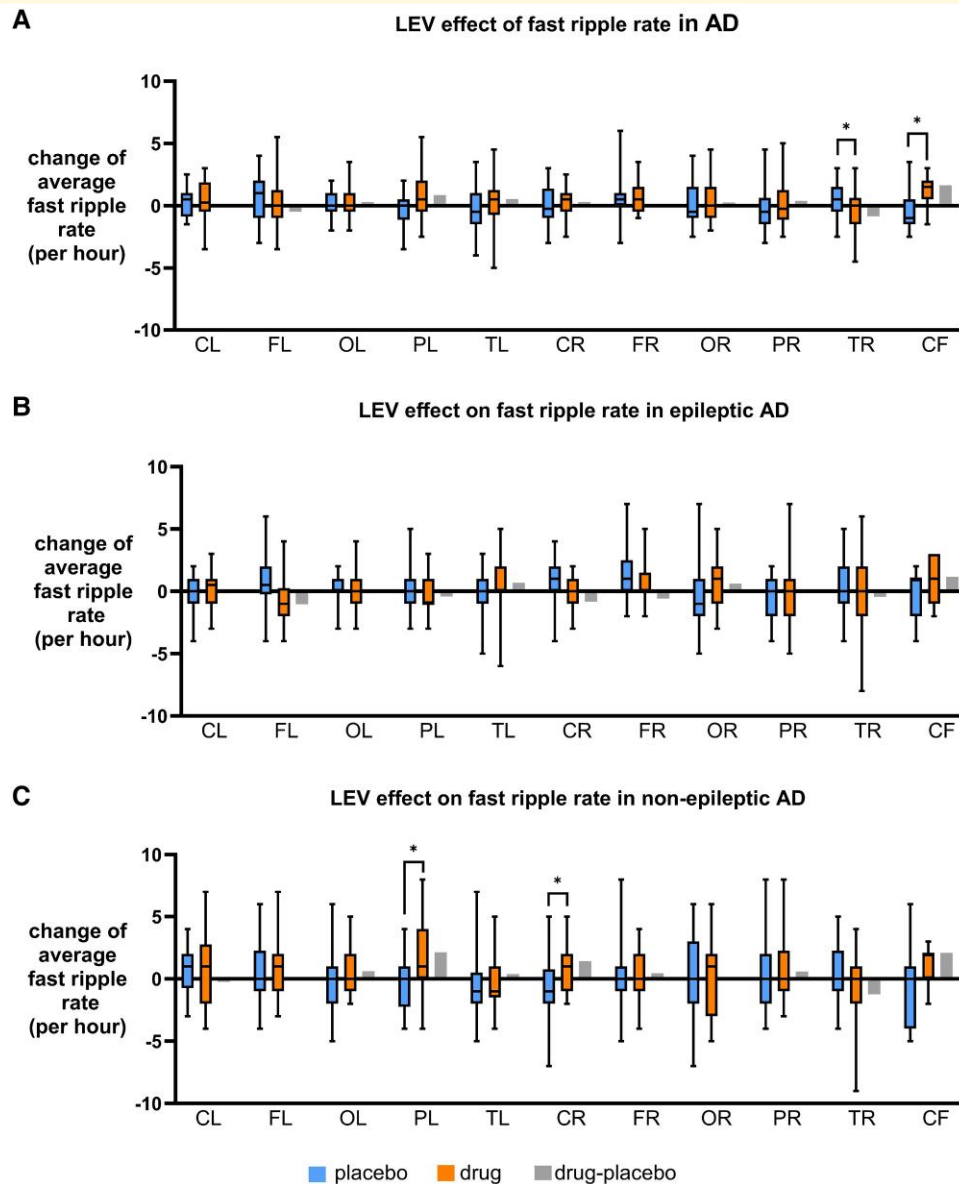


Figure 7 Effect of LEV on FR. (A) Average FRRs per region detected in MEG for Alzheimer's disease before and after LEV treatment are shown in box plot. LEV increased RR in Alzheimer's disease in bilateral parietal and right central but decreased RR in left-frontal and right-occipital regions. (B) Average FRRs per region detected in MEG for EAD before and after LEV treatment are shown in box plot. In EAD, LEV decreased RR in bilateral-frontal and occipital regions and cerebral fissure. (C) Average FRRs per region detected in MEG for NEAD before and after LEV treatment are shown in box plot. In NEAD, LEV increased RR in bilateral parietal and right central regions. $P < 0.05$, unpaired *t*-test or Mann-Whitney test. The average RR or FRR of all participants within a cohort is calculated for each channel, and each regional group of channels is compared between cohorts. Number of channels (**N**) for each region are as follows: CL, central left ($n = 24$); FL, frontal left ($n = 31$); OL, occipital left ($n = 19$); PL, parietal left ($n = 22$); TL, temporal left ($n = 33$); CR, central right ($n = 24$); FR, frontal right ($n = 33$); OR, occipital right ($n = 19$); PR, parietal right ($n = 22$); TR, temporal right ($n = 34$); CF, cerebral fissure ($n = 11$).

line with a previous study in Alzheimer's disease,⁴⁶ which showed that epileptiform discharges detected by MEG were more on the right hemisphere (temporal lobe); whereas EEG detected epileptiform discharges were predominant on the left side. HFOs occur in both awake and sleep states: REM and Non-REM, although their rates are higher in non-REM sleep, followed by awake and then REM sleep.⁵³ R are more affected by sleep/wake state than FR. In our study, there was no difference in participants' awake/sleep

states. FR were present in our control group, who were on average 12 years older than the disease group. While often associated with pathology, FR might also have physiological origins. These findings could potentially represent early signs of hyperexcitability in the aging brain, which might progress to seizure activity. This observation underscores the complexity of distinguishing age-related changes from early pathological processes, suggesting a need for further investigation. We also observed that HFO rates are uncorrelated

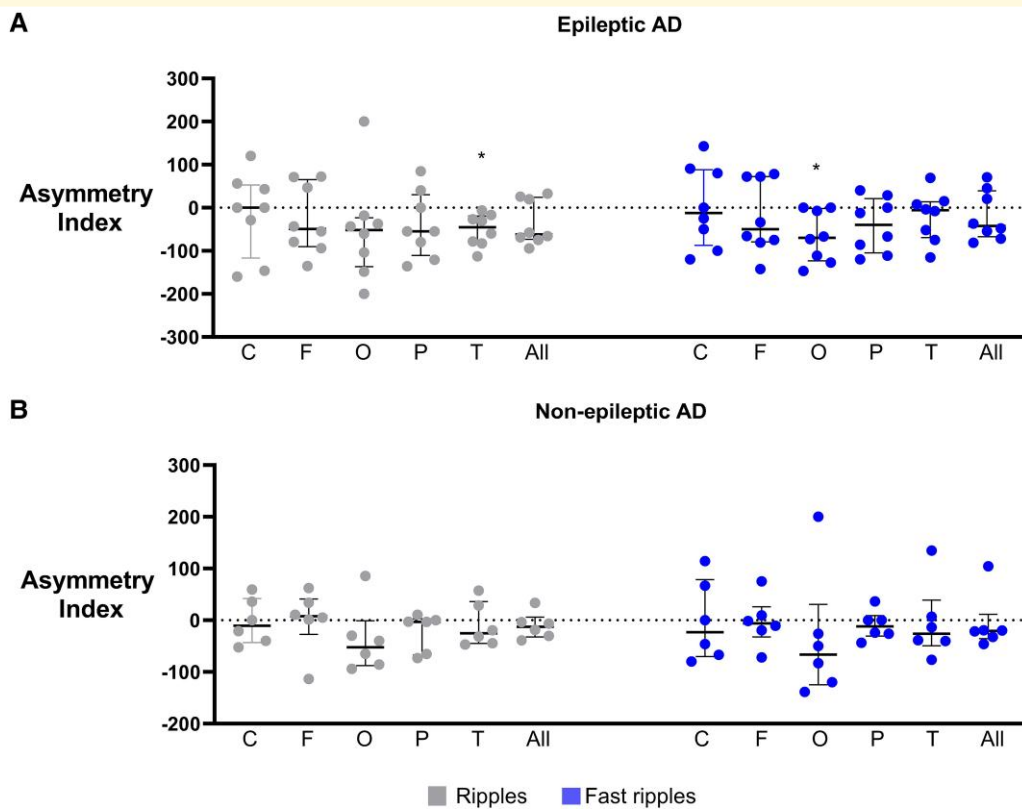


Figure 8 AI of EAD and NEAD. AI of ripples and FR in (A) EAD showed significant asymmetry in occipital and temporal regions, with higher HFOs in the right hemisphere. AI of (B) NEAD shows that there is no asymmetry in any region. $N = 8$ and 6 for EAD and NEAD, respectively. $P < 0.05$, 2-tailed 1-sample t -test versus zero. C, central; F, frontal; O, occipital; P, parietal; T, temporal; All, all regions combined.

across brain regions, leading us to treat each region as independent in our analysis. Future studies should examine inter-regional dependencies before investigating intraregional effects.

We know that LEV can reduce HFOs in the rat model of temporal lobe epilepsy.⁵⁴ In this study, we showed that LEV decreased R HFOs in human epileptic Alzheimer's disease. At our given dose, LEV did not reduce HFOs in all the brain regions that were affected at baseline. It needs to be tested if a different dose can extend LEV's affect across all brain regions in EAD. Surprisingly, LEV differently affected NEAD where it increased the HFOs for both R and FR. This implies that LEV is influencing at least two different mechanisms underlying hyperactivity. This aligns with our previous findings from this same study,⁴ in which, Alzheimer's disease with epileptic activity and Alzheimer's disease without epileptic activity were differently affected by LEV in their measures of cognitive function. For Alzheimer's disease with epileptic activity, compared to placebo, LEV increased performance in the Stroop interference naming test (SINT) and increased learning rates in the virtual route learning test (VRLT), whereas Alzheimer's disease without epileptic activity did not received any benefit from LEV. Compared to Alzheimer's disease without epileptic activity, Alzheimer's disease with epileptic activity had better SINT performance and higher accuracy in VRLT while taking

LEV. One possibility for the differential effects of LEV on HFOs in NEAD and EAD is differences in brain SV2A levels between NEAD and EAD. Brain SV2A levels are decreased in autopsy tissue of epilepsy patients,⁵⁵ and could be more diminished in EAD than in NEAD. Accordingly, LEV's impact could be higher if SV2A levels are lower to start with in EAD. Moreover, the epileptic sub-type of Alzheimer's disease exhibits distinct neurophysiological characteristics particularly in the expression and function of various ion channels and neurotransmitter systems.⁵⁶ These alterations create a unique neural environment that differentiates this sub-type from non-epileptic Alzheimer's disease. Such changes can emerge early in the disease process and can be exacerbated by seizure activity. More insight is needed on the dynamics of synaptic inhibitory processes between the EAD, NEAD and non-AD epileptic systems. Our MEG study captured HFOs that likely represent a mixture of cortical and hippocampal ripples, as MEG sensors aggregate activity from both deep structures and neocortical regions. While our findings demonstrate regional variations in HFO patterns, future studies combining MEG with detailed clinical phenotyping and neuroimaging could help understand whether these patterns differ between Alzheimer's disease variants (e.g. predominantly medial temporal versus neocortical). Additionally, combining MEG with techniques offering higher spatial resolution, such as simultaneous intracranial

EEG, could help distinguish the sources and characteristics of cortical versus hippocampal ripples.

Limitations

The age of control participants was higher than Alzheimer's disease. However, considering pathological nature of HFOs, one could expect their direct relationship with age, but controls had less HFOs. The MEG analysis was limited by noise, and a better signal-to-noise ratio would be more sensitive to detect HFOs by morphology. An HFO study will also benefit from higher sample sizes in more diverse populations. Also, 10-minute M/EEG exams cannot capture all vigilance states in which HFOs can occur. In future studies, longer M/EEG recordings, with high sampling rates, would help to identify HFOs better.

Conclusion and future directions

In this study, we found that Alzheimer's disease exhibited a higher rate of HFOs, with intriguing differences between NEAD and EAD. LEV decreased HFOs in EAD but increased them in NEAD, suggesting that HFOs associated with epileptic activity and asymmetry in Alzheimer's disease are more pathological. Additionally, LEV treatment could increase hyperexcitability in parietal/central regions of non-epileptic Alzheimer's disease cases. While HFOs can serve as a biomarker of hyperexcitability in Alzheimer's disease, their role in Alzheimer's disease pathology and progression requires further investigation. Improved methods for objectively assessing HFOs and handling technique-specific noise, especially for scalp EEG and MEG are needed. Overall, we present strong evidence that HFOs are one of the neurophysiological biomarkers of Alzheimer's disease, and they can be used to study other HFO-correlated molecular and neurophysiological variables in this disease.

Supplementary material

Supplementary material is available at *Brain Communications* online.

Acknowledgements

The authors thank the participants and their family members for giving us the opportunity to study the disease. We thank Dr. David Elashoff, UCLA, for his assistance with determining statistical tests.

Funding

This study was supported by grant PCTRB-13-288476 from the Alzheimer's Association made possible by Part the Cloud

(K.V.), grants R01 NS100440 (S.S.N.), RF1 AG062196 (S.S.N.), R01 DC017696 (S.S.N.), R01 NS033310 (K.V.), R01 AG058820 (K.V.), R01 AG075955 (K.V.) and UH2 AG083254 (K.V.) from the National Institutes of Health and John Douglas French Alzheimer's Foundation (K.V.).

Competing interests

The authors report no competing interests.

Data availability

The data that support the findings of this study are available from the corresponding author, upon reasonable request. The software script is available at <https://github.com/Vossel-Lab/HFO-AD-Lev.git>

References

1. Sherzai D, Losey T, Vega S, Sherzai A. Seizures and dementia in the elderly: Nationwide Inpatient Sample 1999–2008. *Epilepsy Behav.* 2014;36:53-56.
2. Vossel KA, Beagle AJ, Rabinovici GD, *et al.* Seizures and epileptiform activity in the early stages of Alzheimer disease. *JAMA Neurol.* 2013;70(9):1158-1166.
3. Palop JJ, Mucke L. Network abnormalities and interneuron dysfunction in Alzheimer disease. *Nat Rev Neurosci.* 2016;17(12):777-792.
4. Vossel K, Ranasinghe KG, Beagle AJ, *et al.* Effect of levetiracetam on cognition in patients with Alzheimer disease with and without epileptiform activity: A randomized clinical trial. *JAMA Neurol.* 2021;78(11):1345-1354.
5. Sen A, Capelli V, Husain M. Cognition and dementia in older patients with epilepsy. *Brain.* 2018;141(6):1592-1608.
6. Vossel KA, Tartaglia MC, Nygaard HB, Zeman AZ, Miller BL. Epileptic activity in Alzheimer's disease: Causes and clinical relevance. *Lancet Neurol.* 2017;16(4):311-322.
7. Vossel K. Putting the brakes on accelerated cognitive decline in Alzheimer's disease with epileptic activity. *J Alzheimers Dis.* 2023;94(3):1075-1077.
8. Hauteclouque-Raysz G, Sellal F, Bousiges O, Phillipi N, Blanc F, Cretin B. Epileptic prodromal Alzheimer's disease treated with anti-seizure medications: Medium-term outcome of seizures and cognition. *J Alzheimers Dis.* 2023;94(3):1057-1074.
9. Samudra N, Ranasinghe K, Kirsch H, Rankin K, Miller B. Etiology and clinical significance of network hyperexcitability in Alzheimer's disease: Unanswered questions and next steps. *J Alzheimers Dis.* 2023;92(1):13-27.
10. Wu JW, Hussaini SA, Bastille IM, *et al.* Neuronal activity enhances tau propagation and tau pathology in vivo. *Nat Neurosci.* 2016;19(8):1085-1092.
11. Hijazi S, Heistek TS, Scheltens P, *et al.* Early restoration of parvalbumin interneuron activity prevents memory loss and network hyperexcitability in a mouse model of Alzheimer's disease. *Mol Psychiatry.* 2020;25:3380-3398.
12. Styr B, Slutsky I. Imbalance between firing homeostasis and synaptic plasticity drives early-phase Alzheimer's disease. *Nat Neurosci.* 2018;21(4):463-473.
13. Leung H, Zhu CX, Chan DT, *et al.* Ictal high-frequency oscillations and hyperexcitability in refractory epilepsy. *Clin Neurophysiol.* 2015;126(11):2049-2057.

14. Khadjevand F, Cimbalnik J, Worrell GA. Progress and remaining challenges in the application of high frequency oscillations as biomarkers of epileptic brain. *Curr Opin Biomed Eng.* 2017;4:87-96.
15. Jacobs J, Staba R, Asano E, et al. High-frequency oscillations (HFOs) in clinical epilepsy. *Prog Neurobiol.* 2012;98(3):302-315.
16. Frauscher B, Bartolomei F, Kobayashi K, et al. High-frequency oscillations: The state of clinical research. *Epilepsia.* 2017;58(8):1316-1329.
17. Nevalainen P, von Ellenrieder N, Kliměš P, Dubeau F, Frauscher B, Gotman J. Association of fast ripples on intracranial EEG and outcomes after epilepsy surgery. *Neurology.* 2020;95:e2235-e2245.
18. Fedele T, Burnos S, Boran E, et al. Resection of high frequency oscillations predicts seizure outcome in the individual patient. *Sci Rep.* 2017;7(1):13836.
19. Hussain SA, Mathern GW, Hung P, Weng J, Sankar R, Wu JY. Intraoperative fast ripples independently predict postsurgical epilepsy outcome: Comparison with other electrocorticographic phenomena. *Epilepsy Res.* 2017;135:79-86.
20. Qi L, Fan X, Tao X, et al. Identifying the epileptogenic zone with the relative strength of high-frequency oscillation: A stereoelectroencephalography study. *Front Hum Neurosci.* 2020;14:186.
21. Thomschewski A, Hincapié AS, Frauscher B. Localization of the epileptogenic zone using high frequency oscillations. *Front Neurol.* 2019;10:94.
22. Huang CM, White LE Jr. High-frequency components in epileptiform EEG. *J Neurosci Methods.* 1989;30:197-201.
23. Bragin A, Engel J Jr, Wilson CL, Fried I, Mathern GW. Hippocampal and entorhinal cortex high-frequency oscillations (100–500 Hz) in human epileptic brain and in kainic acid-treated rats with chronic seizures. *Epilepsia.* 1999;40:127-137.
24. Bragin A Jr, Engel J, Wilson CL, Vizenin E, Mathern GW. Electrophysiologic analysis of a chronic seizure model after unilateral hippocampal KA injection. *Epilepsia.* 1999;40:1210-1221.
25. Fisher RS, Webber WR, Lesser RP, Arroyo S, Uematsu S. High-frequency EEG activity at the start of seizures. *J Clin Neurophysiol.* 1992;9:441-448.
26. Bragin A, Engel J Jr, Wilson CL, Fried I, Buzsáki G. High frequency oscillations in human brain. *Hippocampus.* 1999;9:137-142.
27. Brázdil M, Pail M, Haláček J, et al. Very high-frequency oscillations: Novel biomarkers of the epileptogenic zone. *Ann Neurol.* 2017;82(2):299-310.
28. Usui N, Terada K, Baba K, et al. Significance of very-high-frequency oscillations (over 1,000 Hz) in epilepsy. *Ann Neurol.* 2015;78(2):295-302.
29. Chen Z, Maturana MI, Burkitt AN, Cook MJ, Grayden DB. High-frequency oscillations in epilepsy: What have we learned and what needs to be addressed. *Neurology.* 2021;96(9):439-448.
30. Jirsch JD, Urrestarazu E, LeVan P, Olivier A, Dubeau F, Gotman J. High-frequency oscillations during human focal seizures. *Brain.* 2006;129:1593-1608.
31. Zijlmans M, Worrell GA, Dümpelmann M, et al. How to record high-frequency oscillations in epilepsy: A practical guideline. *Epilepsia.* 2017;58(8):1305-1315.
32. Ngo H-V, Fell J, Staresina B. Sleep spindles mediate hippocampal-neocortical coupling during long-duration ripples. *eLife.* 2020;9:e57011.
33. Jiang X, Gonzalez-Martinez J, Halgren E. Coordination of human hippocampal sharpwave ripples during NREM sleep with cortical theta bursts, spindles, downstates, and upstates. *J Neurosci.* 2019;39:8744-8761.
34. Khodagholy D, Gelinás JN, Buzsáki G. Learning-enhanced coupling between ripple oscillations in association cortices and hippocampus. *Science.* 2017;358:369-372.
35. Vaz AP, Inati SK, Brunel N, Zaghoul KA. Coupled ripple oscillations between the medial temporal lobe and neocortex retrieve human memory. *Science.* 2019;363:975-978.
36. Cimbalnik J, Brinkmann B, Kremen V, et al. Physiological and pathological high frequency oscillations in focal epilepsy. *Ann Clin Transl Neurol.* 2018;5(9):1062-1076.
37. Frauscher B, von Ellenrieder N, Zelmann R, et al. High-Frequency oscillations in the normal human brain. *Ann Neurol.* 2018;84(3):374-385.
38. Kerber K, Dümpelmann M, Schelter B, et al. Differentiation of specific ripple patterns helps to identify epileptogenic areas for surgical procedures. *Clin Neurophysiol.* 2014;125(7):1339-1345.
39. Jacobs J, LeVan P, Chander R, Hall J, Dubeau F, Gotman J. Interictal high-frequency oscillations (80–500 Hz) are an indicator of seizure onset areas independent of spikes in the human epileptic brain. *Epilepsia.* 2008;49(11):1893-1907.
40. Staba RJ, Wilson CL, Bragin A, Fried I, Engel J Jr. Quantitative analysis of high-frequency oscillations (80–500 Hz) recorded in human epileptic hippocampus and entorhinal cortex. *J Neurophysiol.* 2002;88(4):1743-1752.
41. Staba RJ, Frigetto L, Behnke EJ, et al. Increased fast ripple to ripple ratios correlate with reduced hippocampal volumes and neuron loss in temporal lobe epilepsy patients. *Epilepsia.* 2007;48(11):2130-2138.
42. Pail M, Cimbalnik J, Roman R, et al. High frequency oscillations in epileptic and non-epileptic human hippocampus during a cognitive task. *Sci Rep.* 2020;10(1):18147.
43. Garrett JC, Verzhbinsky IA, Kaestner E, et al. Binding of cortical functional modules by synchronous high-frequency oscillations. *Nat Hum Behav.* 2024;8(10):1988-2002.
44. Papadelis C, Tamilia E, Stufflebeam S, et al. Interictal high frequency oscillations detected with simultaneous magnetoencephalography and electroencephalography as biomarker of pediatric epilepsy. *J Vis Exp.* 2016;(118):54883.
45. World Medical Association. World Medical Association Declaration of Helsinki: Ethical principles for medical research involving human subjects. *JAMA.* 2013;310(20):2191-2194.
46. Vossel KA, Ranasinghe KG, Beagle AJ, et al. Incidence and impact of subclinical epileptiform activity in Alzheimer's disease. *Ann Neurol.* 2016;80(6):858-870.
47. Roehri N, Lina JM, Mosher JC, Bartolomei F, Benar CG. Time-frequency strategies for increasing high-frequency oscillation detectability in intracerebral EEG. *IEEE Trans Biomed Eng.* 2016;63(12):2595-2606.
48. Roehri N, Pizzo F, Bartolomei F, Wendling F, Bénar CG. What are the assets and weaknesses of HFO detectors? A benchmark framework based on realistic simulations. *PLoS One.* 2017;12(4):e0174702.
49. Knopman DS, Amieva H, Petersen RC, et al. Alzheimer disease. *Nat Rev Dis Primers.* 2021;7:33.
50. Lisgaras CP, Scharfman HE. High-frequency oscillations (250–500 Hz) in animal models of Alzheimer's disease and two animal models of epilepsy. *Epilepsia.* 2023;64(1):231-246.
51. Beal MF, Mazurek MF, Chartha GK, Svendsen CN, Bird ED, Martin JB. Neuropeptide Y immunoreactivity is reduced in cerebral cortex in Alzheimer's disease. *Ann Neurol.* 1986;20(3):282-288.
52. Takahashi M, Hayashi S, Kakita A, et al. Patients with temporal lobe epilepsy show an increase in brain-derived neurotrophic factor protein and its correlation with neuropeptide Y. *Brain Res.* 1999;818(2):579-582.
53. Staba RJ, Wilson CL, Bragin A, Jhung D, Fried I, Engel J Jr. High-frequency oscillations recorded in human medial temporal lobe during sleep. *Ann Neurol.* 2004;56(1):108-115.
54. Lévesque M, Behr C, Avoli M. The anti-ictogenic effects of levetiracetam are mirrored by interictal spiking and high-frequency oscillation changes in a model of temporal lobe epilepsy. *Seizure.* 2015;25:18-25.
55. van Vliet EA, Aronica E, Redeker S, Boer K, Gorter JA. Decreased expression of synaptic vesicle protein 2A, the binding site for levetiracetam, during epileptogenesis and chronic epilepsy. *Epilepsia.* 2009;50(3):422-433.
56. Barbour AJ, Gourmaud S, Lancaster E, et al. Seizures exacerbate excitatory: Inhibitory imbalance in Alzheimer's disease and 5XFAD mice. *Brain.* 2024;147(6):2169-2184.